NPL
National Physical Laboratory

NPL REPORT MAT 137

INTERLABORATORY COMPARISON OF STRAIN MEASUREMENT BY HIGH RESOLUTION ELECTRON BACKSCATTER DIFFRACTION

V. TONG, K. P. MINGARD,

F. ADAMSKI, B. BEAUSIR, J. BRUCKBAUER, G. CIOS, D. DINGLEY, D. FULLWOOD, S. KALACSKA, A. KOKO, M. MCLEAN, W. OSBORN, N. RADI, A. SCHWEDT, Q. SHI, B. STACEY, Y. WANG, A. WINKELMANN

MARCH 2026

INTERLABORATORY COMPARISON OF STRAIN MEASUREMENT BY HIGH RESOLUTION ELECTRON BACKSCATTER DIFFRACTION

V. Tong and K.P. Mingard
Materials and Mechanical Metrology, National Physical Laboratory

F. Adamski[1], B. Beausir[2], J. Bruckbauer[3], G. Cios[4], D. Dingley[5], D. Fullwood[6], S. Kalacska[7], A. Koko[8], M. McLean[9], W. Osborn[9], N. Radi[1], A. Schwedt[10], Q. Shi[11], B. Stacey[5], Y. Wang[12], A. Winkelmann[3]

1. Safran Tech, France
2. ATEX Software (www.atex-software.eu)
3. University of Strathclyde, UK
4. AGH University of Krakow, Poland
5. BLG Vantage (www.hrebsd.com)
6. Brigham Young University, USA
7. CNRS École des Mines de Saint-Etienne, France
8. National Physical Laboratory, UK
9. National Institute of Standards and Technology, USA
   Will Osborn ORCID: 0000-0003-4238-4893
   Mark McLean ORCID: 0000-0003-0336-5972
10. RWTH Aachen, Germany
11. Shanghai Jiao Tong University, China
12. Independent researcher

ABSTRACT

An interlaboratory comparison (ILC) has been conducted to evaluate the data analysis uncertainty component from High angular Resolution Electron BackScatter Diffraction (HR-EBSD) elastic strain measurements. Fourteen participants in the ILC performed HR-EBSD analysis on identical sets of data acquired at NPL and NIST, from a Si-SiGe candidate reference material with independently measured tetragonal elastic strains. The elastic strain uncertainty is on the order of ± 10^{-4} in unstrained crystal and ± 10^{-3} in strained crystal, and likely dominated by systematic errors in pattern centre location. Recommendations are given for how to measure and report strain uncertainty in HR-EBSD, as well as potential topics and design of follow-on ILCs.

ISSN 1754-2979

https://doi.org/10.47120/npl.MAT137

National Physical Laboratory
Hampton Road, Teddington, Middlesex, TW11 0LW

The work at NPL was funded by the UK Government's Department for Science, Innovation & Technology through the UK's National Measurement System programmes.

Approved on behalf of NPL by
Stefanos Giannis, Science Area Leader

CONTENTS

1 INTRODUCTION

High Resolution Electron BackScatter Diffraction or HR-EBSD is a method originally developed by Wilkinson, Meaden and Dingley [1] for measuring very small changes in backscatter diffraction patterns (EBSPs) to determine elastic strains and lattice rotations with a precision of approximately 10^{-4} for strain. The high resolution thus refers to high angular resolution, rather than lateral resolution between measurement positions, the latter being determined by the electron interaction volume.

The capability to measure strain with this level of precision enables calculation of residual stress at the microstructural level. This in turn enables, for example, understanding the effects of precipitates or grain boundaries on strengthening materials [2], [3]. The angular precision also allows mapping of the distribution of geometrically necessary dislocation density since changes in orientation within a crystal must result from the presence of these defects. The technique has been applied to analysis of both semiconductor devices and structural materials (metals, ceramics).

Both the acquisition of the EBSPs and the subsequent processing of them involve a large number of variables which must be carefully controlled if high precision is to be achieved. When EBSD based strain measurements are made compared to an experimental reference pattern, the measured strains are relative to the reference pattern. It is convenient for the reference pattern to be taken from an unstrained region of the sample which can be hard to achieve, particularly in polycrystalline samples. Even putting this to one side, there are still a large number of experimental and computational issues that need to be considered.

2 STANDARDISATION NEEDS

Individual studies (e.g. [4]) have looked at the effect of experimental parameters on achieving higher precision. Reference [5] reviews a large number of publications that have investigated this and particularly the effect of reference pattern selection. Before any standardisation of the technique can be considered, a better understanding is needed of the way in which variables in the acquisition and analysis are employed by different users with different equipment. Even with the same equipment, multiple image analysis methods are available through commercial, open-source and in-house software packages.

Currently there is little data to show how reproducible the basic technique can be as most reported data in the scientific literature is from a single source.

Experimental issues that can affect the precision level and repeatability and reproducibility of HR-EBSD include:

- Quality (noise, resolution) of EBSPs
- Calibration of microscope and detector geometry that acquired the EBSPs (including the pattern centre position and beam shift effects)
- Choice of reference pattern (how close it is to zero strain, how corrections are made for selection of different positions)

The above are also quite apart from the quality of the sample preparation and polishing.

Even assuming the above factors are well controlled, or that a single set of patterns is acquired for analysis, a number of factors in the calculations and software used to analyse the patterns have been known to lead to different results, including:

- Different algorithms used by different groups
- Different release versions of the most commonly available commercial software (improvements and bug fixes have resulted in multiple releases) are known to output different results

- Within each software package, many parameters can be adjusted for the patterns available and the material under analysis and can lead to different results, but decisions on how to adjust these parameters is open to user interpretation.
- There can be interface issues between experiment and analysis caused by different descriptions of parameters by the separate analysis and acquisition software packages.

The most straightforward starting point to investigate reproducibility is to examine just the computational analysis part of the process: calculations by different groups with a variety of software packages, from a single set of patterns at least eliminates the experimental acquisition variables, and can be organised without the need to source and distribute multiple samples or circulate a single sample.

3 INTERLABORATORY COMPARISON

An interlaboratory comparison has been set up under the auspices of VAMAS Technical Working Area 37.

3.1 SAMPLE

HR-EBSD data for analysis by the participants in the ILC were acquired from candidate reference materials which consists of alternating bands of Si and Si-Ge grown epitaxially on the Si (Figure 1). The change in unit cell dimensions at the interface induces a tetragonal strain of SiGe relative to cubic Si that depends only on Ge concentration, as long as the SiGe layer is thin enough to remain coherent at the Si/SiGe interface. This strain can be measured independently using HR-EBSD and X-ray diffraction (XRD) techniques. The analytical framework for comparing XRD to HR-EBSD measurements on similar materials were developed and reported by NIST [6].

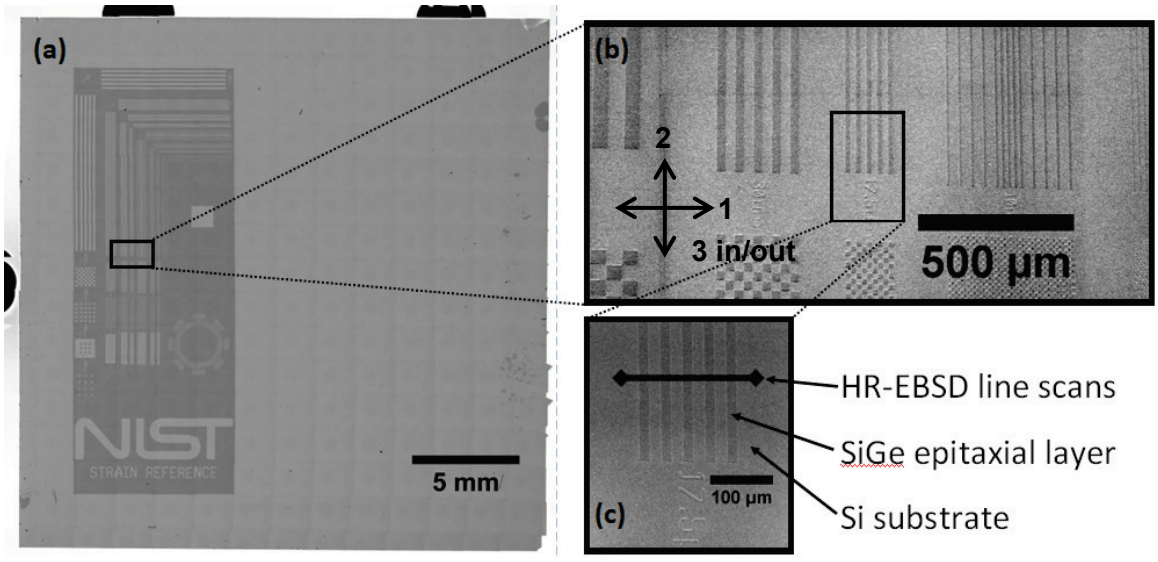

Figure 1: (a) RM8191 Si-SiGe candidate reference material developed at NIST; (b) Si-SiGe lines with tetragonal elastic strains; (c) HR-EBSD line scan region of interest on 17.5 µm lines. The 1, 2 and 3 sample directions are labelled with double-headed arrows because the +/- sense of the HR-EBSD line scans with respect to the chip orientations were not controlled. This ambiguity does not affect the results because the sample is similarly symmetric. The 1, 2 and 3 directions form a right-handed set.

3.2 REFERENCE STRAINS

Six HR-EBSD line-scans were acquired from Si/SiGe chips cut from two wafers with different nominal SiGe compositions (Wafer b- and a-), using three combinations of SEM-EBSD equipment: one SEM-EBSD system at NPL (NPL1) and two SEM-EBSD systems at NIST (NIST1, NIST2).

Table 1 shows the reference strains which will be used to compare to HR-EBSD measured strains. The reference normal strain components, $\boldsymbol{\varepsilon}_{11}^{Ref}$, $\boldsymbol{\varepsilon}_{22}^{Ref}$ and $\boldsymbol{\varepsilon}_{33}^{Ref}$ are directly comparable to the corresponding strain tensor components measured from HR-EBSD.

Reference strains were measured from each individual chip using HR-XRD measurements of the Si and SiGe (004) planes for SiGe relative to Si. The SiGe compositions and tetragonal strains were determined from lattice parameters tabulated in Reference [7] and the analytical framework described in Reference [6]. The reference tetragonal strains, $\boldsymbol{\varepsilon}_{\boldsymbol{T}}^{Ref}$, have uncertainties on the order of ± 10^{-5}.

Table 1: Reference strain values from theoretical prediction and HR-XRD measurements.

	Data1	**Data2**	**Data3**	**Data4**	**Data5**	**Data6**
Si/SiGe wafer-chip ID	b-B07	b-C04	b-C04	a-C03	a-G05	b-C04
SEM-EBSD system	NPL1	NIST1	NIST2	NIST1	NPL1	NIST2
SiGe composition [Ge atom %]	28.2	28.3	28.3	18.9	19.4	28.3
$\boldsymbol{\varepsilon}_{11}^{Ref}$ [10^{-3}]	-10.67	-10.72	-10.72	-7.09	-7.30	-10.72
$\boldsymbol{\varepsilon}_{22}^{Ref}$ [10^{-3}]	-10.67	-10.72	-10.72	-7.09	-7.30	-10.72
$\boldsymbol{\varepsilon}_{33}^{Ref}$ [10^{-3}]	8.18	8.22	8.22	5.44	5.60	8.22
$\boldsymbol{\varepsilon}_{\boldsymbol{T}}^{Ref}$ [10^{-3}]	18.85	18.94	18.94	12.53	12.90	18.94

3.3 PARTICIPANTS

The experimental data were made available to 26 participants for calculation of the elastic strains with their own HR-EBSD analysis software and in-house protocol with a request to complete the reporting template in Appendix 1.

Results returned from 16 participants have been grouped according to the HR-EBSD analysis method (A-G): participants A1 – A10 all used the same general software, but a range of different versions and analysis parameters. Participants B1 – G1 used different software packages and/or methods for measuring relative elastic strains from EBSD patterns.

A range of analysis methods and software types are represented: three are commercially available, one is open-source, and the rest are closed-source programs developed and maintained by individual research groups. Analysis methods include: different digital image correlation techniques to measure EBSD pattern distortions, different models for fitting EBSD pattern distortions to crystal deformations, and use of either experimental or simulated EBSD patterns as a strain-free reference.

4 RESULTS

4.1 NORMAL STRAIN COMPONENTS

Figure 2 shows an typical example of HR-EBSD output data: the normal strain components from all six line scans (Data1 – Data6) returned by participant A3. The reference values of normal strain components are zero for the Si phase, and non-zero (marked by black dashed lines) for the SiGe phase.

Systematic errors between SEM-EBSD systems can be observed. Data1 and Data5, acquired using system NPL1, show a non-zero ε_{22} strain gradient across the five SiGe stripes, and larger errors in ε_{22} than ε_{11}. This deviation from the expected square-wave profile is most likely caused by a misalignment between specimen tilt axis and beam scan direction, and a corresponding error in pattern centre coordinates. Data3 and Data6, acquired from the same chip using system NIST2, show large, repeatable overestimations compared the other two datasets from the same wafer and the reference values. The SEM image pixel size for system NPL1 appears to be slightly smaller than the two NIST systems, and can be observed as a horizontal offset between the line profiles. This is likely caused by a difference in SEM pixel size calibration and affects the calibrated effective pixel size of the EBSD detector.

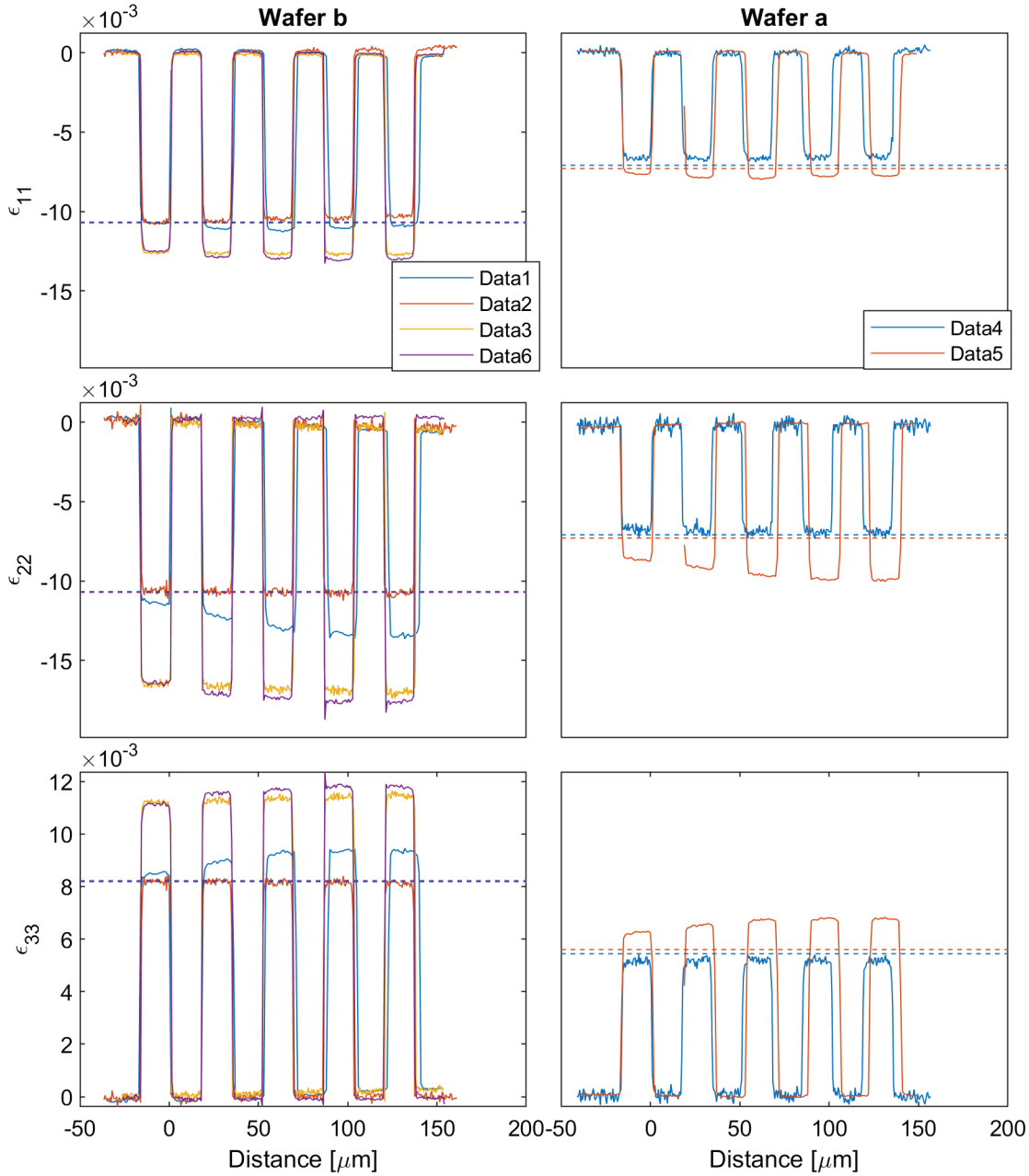

Figure 2: Example normal strain components for all six line-scan datasets (HR-EBSD analysis from participant A3) compared to their reference values, which are plotted as dashed lines in the same colour as their respective HR-EBSD line-scans (the reference values for the chips from Wafer b are so similar that the dashed lines are inseparable in this figure). Line scans were acquired at various step sizes between 0.39 µm and 1 µm, so differences in high-frequency noise are not directly comparable between datasets.

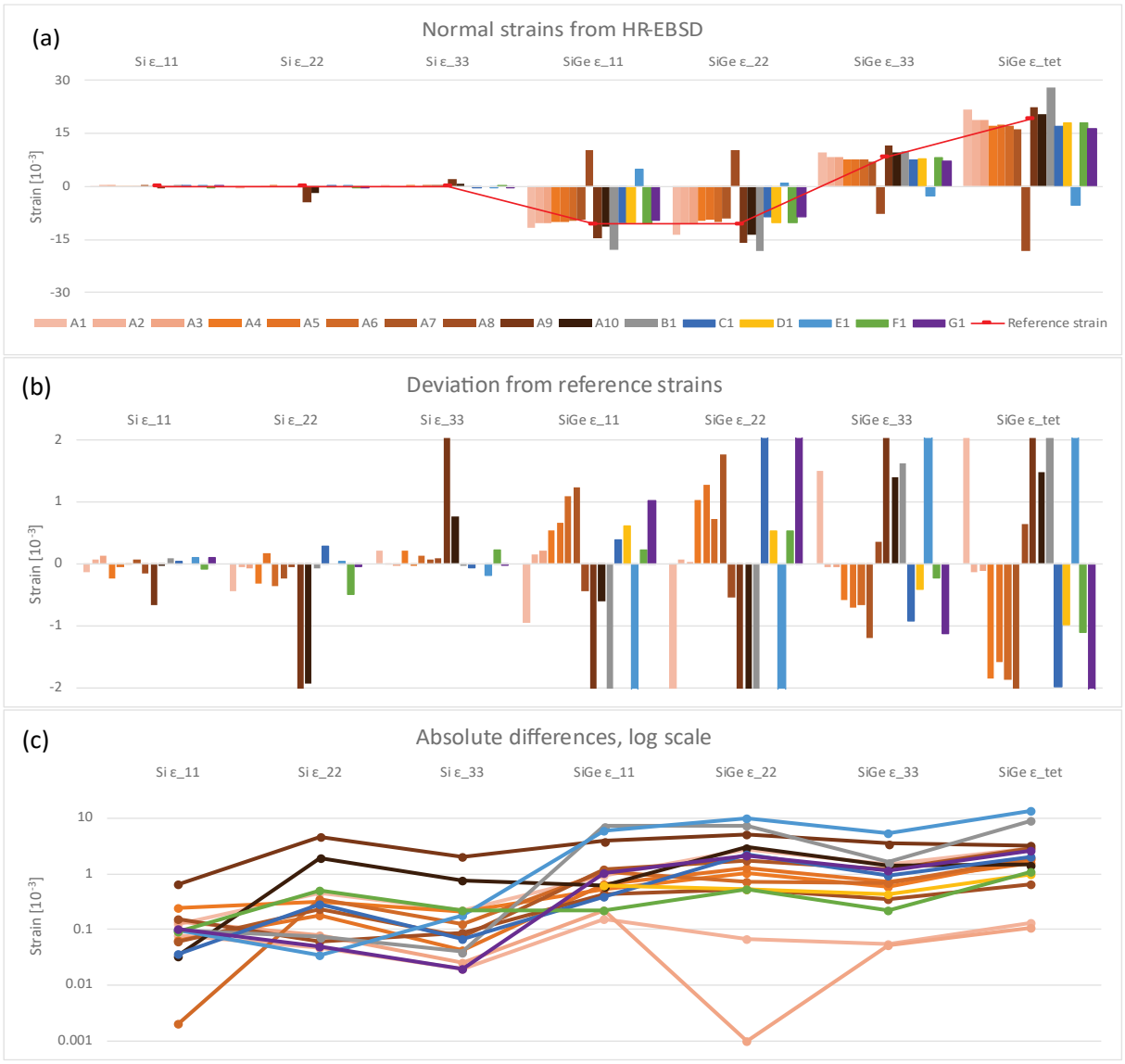

Figure 3: Normal strain components of line scan Data2. (a) Reported HR-EBSD normal strains; (b) deviations from reference strain values; (c) absolute values of (b) plotted on a log scale. Lines are drawn between markers in (a) and (c) only to group similar datasets. The vertical scale showing deviation from reference strain in (b) is clipped to ± 2 × 10^{-3} even though the full range of the data goes up to ± 13 × 10^{-3}, as shown in the equivalent log-scale plot in (c).

Figure 3(a) compares the average normal strain components calculated by all ILC participants (bars) with reference values (markers connected by a line) for one of the line scans (Data2 was chosen because it was the only dataset for which all participants submitted a report). Figure 3(b) and (c) shows the strain errors as deviations between measured and reference strains on linear and log scales respectively.

The HR-EBSD normal strain error is on the order of ± 10^{-4} in the Si phase, which have reference strains of zero, but increases to ± 10^{-3} in SiGe, which have reference strains on the order of ± 10^{-2} (see Table 1 for details). The scatter in SiGe strain error are similar in the higher-strain (Data1, 2, 3, 6) and lower-strain (Data4, 5) SiGe materials.

All participants except for A8 and E1 reported strain values that followed the same broad trends. Participant E1 reported strains with opposite signs and incorrect magnitudes. Participant A8 reported strains with approximately correct magnitudes but opposite signs

(Figure 3(a)), and detailed inspection of their report showed that a SiGe EBSD pattern had been used as the zero-strain reference. Therefore, the signs were flipped for the purposes of comparing to the reference strain values (Figure 3(b) and (c), Figure 4), which is a valid approximation for small strains (i.e. an infinitesimal deformation framework). Participant A5 also reported strain values which were consistently 10^{-3} too small; these were handled as a minor reporting units error (strain vs millistrain) and fixed silently.

Most methods report similar strain magnitudes, except for outliers in methods B and E.

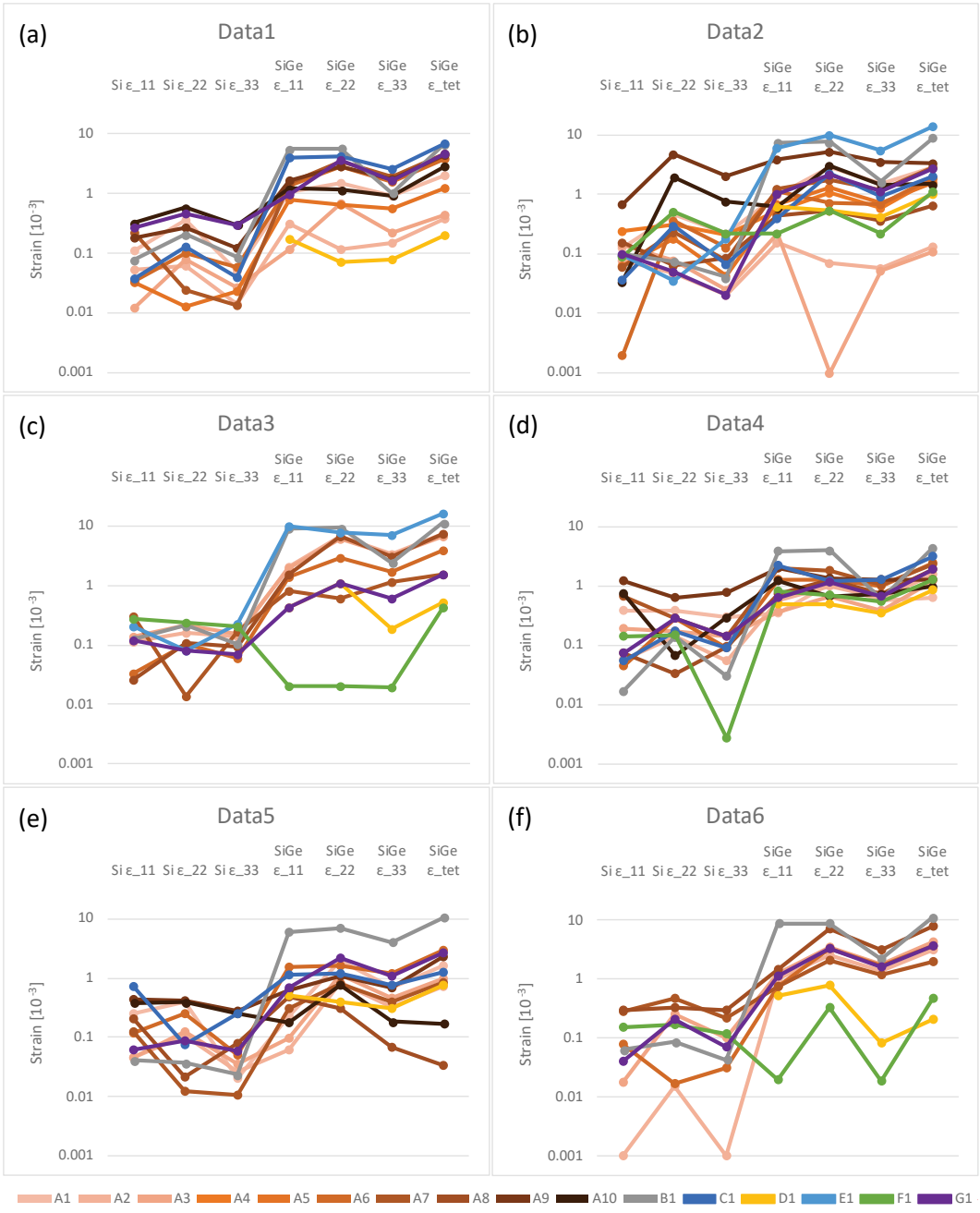

Figure 4: HR-EBSD strain errors for normal strain components, for all six line scans, plotted on a log scale.

4.2 SHEAR STRAIN AND OUT-OF-PLANE SHEAR STRESS COMPONENTS

HR-EBSD calculates elastic strains by finding the best-fit deformation gradient tensor to match the distortion of an EBSD pattern with respect to a reference. However, crystal deformation is not the only cause of EBSD pattern distortions; they can also arise from small changes to the sample position (i.e. electron beam shift) with respect to the EBSD detector, i.e. the pattern centre coordinates (PC = [PC_1, PC_2, PC_3]).

The PC movement as the SEM beam scans across the sample can be compensated for by assuming that the surface is planar and well-aligned to the SEM stage axes, and the EBSD detector pixel size is known. Uncertainties in EBSD pattern or electron probe position, such as from detector instability or distortion [8], sample surface topography, or misalignment of the sample relative to SEM stage axes, can contribute to PC position uncertainties, which in turn lead to uncertainties in the projective transformation between the crystal lattice and EBSD pattern. Since a projective transform can appear very similar in form to crystal deformation, a miscalibrated PC can lead to “phantom” out-of-plane strain components in HR-EBSD [9].

Non-zero out-of-plane stresses are usually errors in HR-EBSD, since the EBSD probe depth is very close to the sample surface. In many HR-EBSD methods, a traction-free surface condition assumption is used, with the crystal’s anisotropic elastic constants, to calculate the hydrostatic strain component which is not visible directly as an EBSD pattern distortion [1]. In practical implementations of this method, the out-of-plane normal stresses σ_{33} are assumed to be zero to allow the trace of the deformation tensor to be solved, but the out-of-plane shear stress components are not numerically constrained but should also be very close to zero if the HR-EBSD calculation is reliable and as long as the traction-free surface assumption is valid, i.e. the specimen surface is relatively flat (≤ 475 nm height change over an in-plane length scale of 10 µm) and well-aligned to (≤ ± 2.7°) the SEM stage axes. This is true for the present experimental data, and also generally applicable to most material types prepared to a standard metallographic finish [10].

Therefore, out-of-plane shear stresses can be used as a measure of the HR-EBSD strain calculation quality. Out-of-plane shear stresses are easier to interpret than the corresponding strain and rotation components, which can arise from either PC errors or genuine crystal strains and rotations, but the unit conversion between errors in stresses to elastic strains may not be trivial.

For the NIST Si/SiGe reference material, the reference values of shear strain and stress components are zero for both Si and SiGe, although the total strain of the SiGe phase is not zero. Errors in PC_1 (component parallel to the SEM stage tilt axis and HR-EBSD line-scan direction) lead to systematic errors in ε_{31} and σ_{31}, and errors in PC_2 (component parallel to the SEM stage tilt direction and perpendicular to the line-scan direction) leads to systematic errors in ε_{32} and σ_{32} [9].

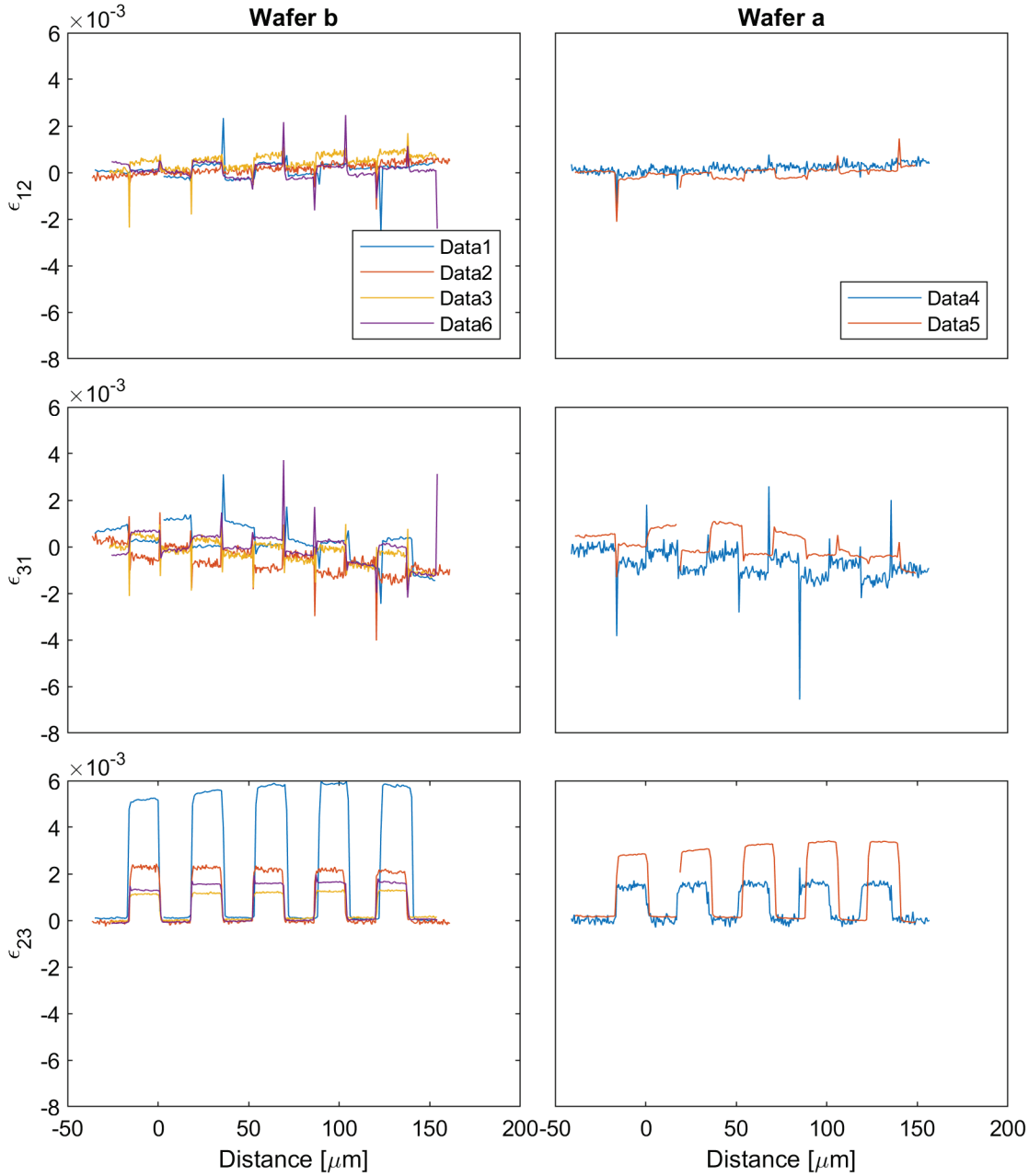

Figure 5: Example shear strain components for all six line scan datasets (participant A3). Sharp spikes near Si/SiGe stripe boundaries are likely artefacts caused by the stripe height shadowing portions of the EBSD detector.

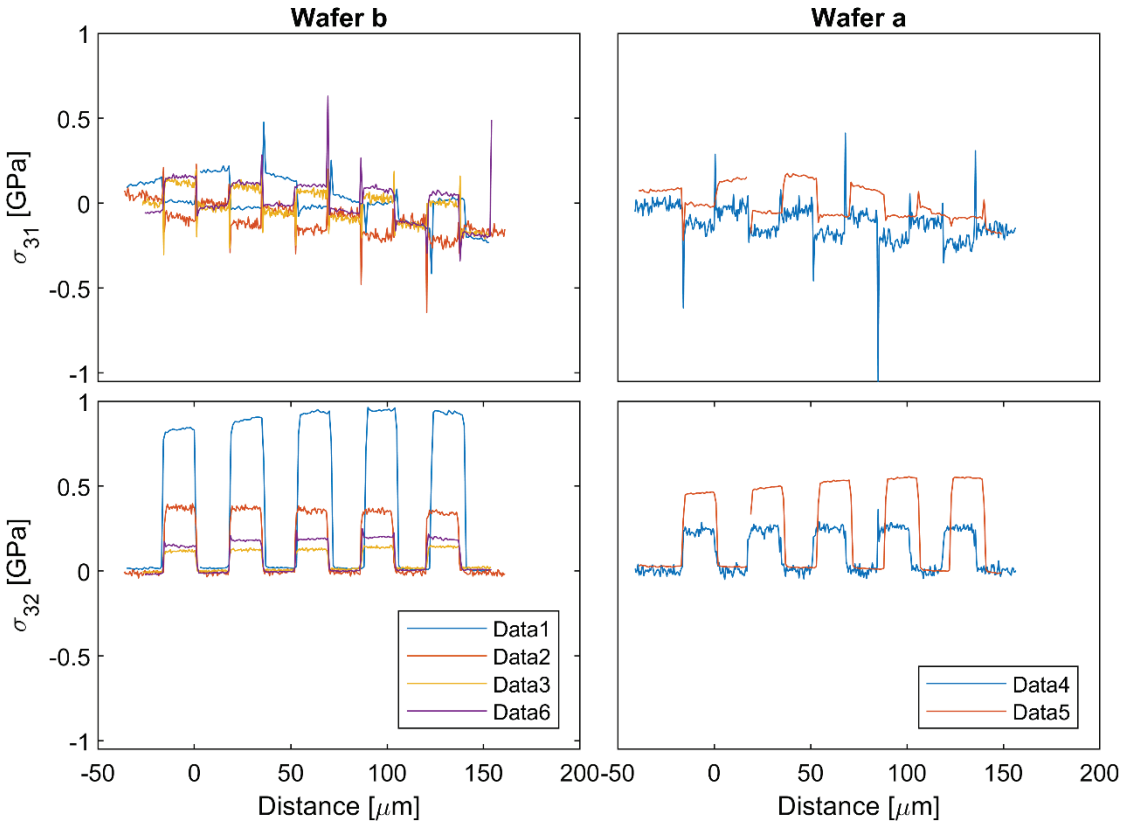

Figure 6: Example out-of-plane shear stress components for all six line scan datasets (participant A3).

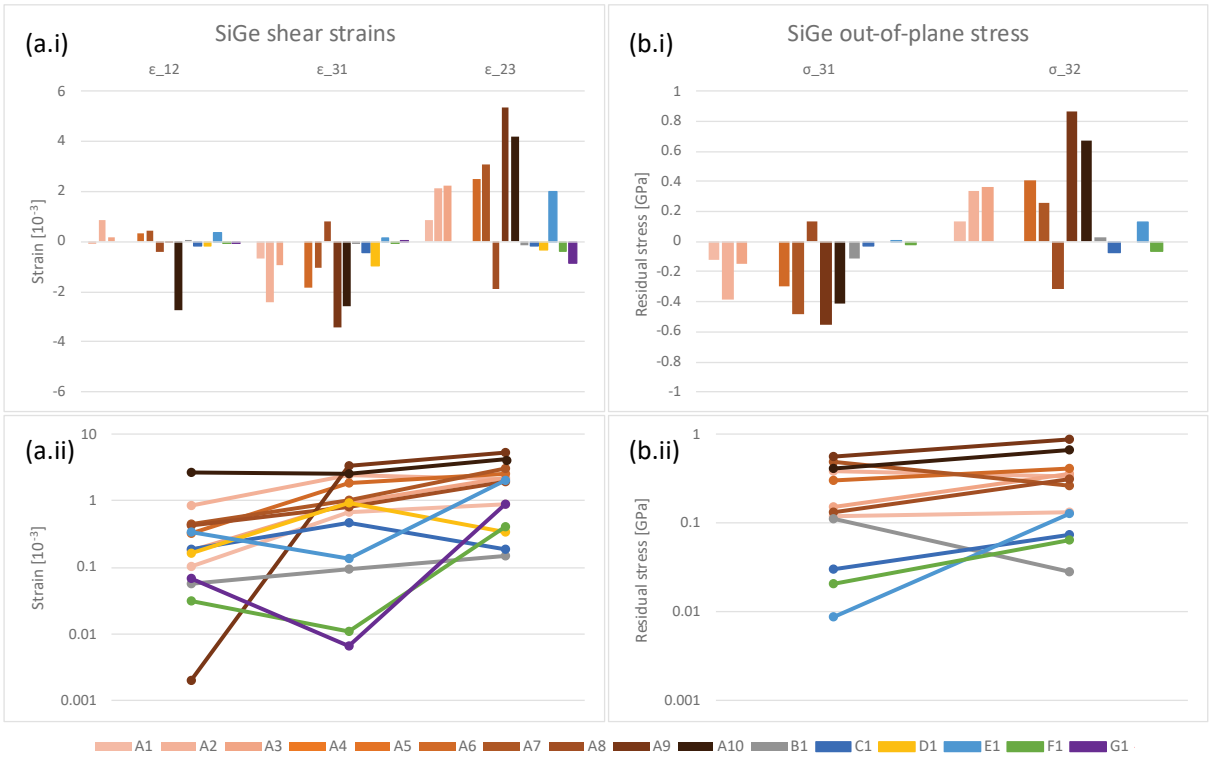

Figure 7: (a) Shear strain (error) components of line scan Data2, plotted on (i) linear and (ii) log scales. (b) Out-of-plane shear stress (error) components of line scan Data2, plotted on (i) linear and (ii) log scales. Missing bars are where no data was reported, either because these strain components were not calculated due to method limitations, or because of participant omission.

Figure 5 and Figure 6 show line profiles of out-of-plane shear stress and strain components. These show errors in PC calibration for each experiment, since the reference SiGe shear strains near the SiGe stripe interiors are zero[1]. Corresponding components have similar line profiles, and all of them follow the Si/SiGe stripe pattern. PC errors in the Si phase remain near-zero, but the SiGe phase shows large phantom stresses and strains, and their magnitudes are grouped by SEM-EBSD system (see Table 1).

PC_2 errors appear to be larger than PC_1 errors, particularly for line scans Data1 and Data5 from SEM-EBSD system NPL1, and the corresponding phantom stresses are larger and more closely follow the shape of the Si/SiGe stripes. The etch depth of SiGe lines was less than 75 nm, i.e. the surface height change between SiGe and Si stripes had a negligible effect on PC.

Figure 7(a) shows that the SiGe out-of-plane shear strain errors are, on average, around $\pm 10^{-3}$ for line scan Data2. Analysis of normal strain components in the previous section (4.1) showed a strain error of around $\pm 10^{-4}$ when the reference value is zero, and 10^{-3} when the reference value is non-zero. The reference SiGe shear strains are zero but the total strain in the SiGe phase is non-zero, and the shear strain errors are around $\pm 10^{-3}$, similar to the normal strain errors.

Figure 7(b) shows the SiGe out-of-plane shear stress components, which also have a reference value of zero. They are, on average, around ± 0.2 GPa for line scan Data2, but much larger when the PC errors is large: up to ± 1 GPa for Data1.

Figure 8 and Figure 9 compare all six HR-EBSD datasets with corresponding plots to Figure 7(a) and Figure 7(b) respectively, which only showed results for Data2. Positive correlations between the error magnitudes for all strain types can be observed for all datasets analysed with method A, i.e. datasets with larger shear strain and stress errors also have larger normal stress errors (Figure 4). This is also the case for Data3 and Data6, which participant A3's report showed anomalously low out-of-plane shear stresses (Figure 6) even though the normal strain errors were large (Figure 2). (There was insufficient input data to perform an equivalent error correlation analysis for methods B – G, which had only one participant each.)

Figure 8 and Figure 9 show that strong correlations in the average out-of-plane shear strain and stress components are present for method A (1 – 8): $\varepsilon_{12} < -\varepsilon_{31} < \varepsilon_{23}$, and $-\sigma_{31} \approx \sigma_{23}$. In the case of participant A8, who used a SiGe instead of Si reference EBSD pattern, the signs of the shear strains and stresses are flipped with respect to the other Method A returns, but the signs of the out-of-plane shear stresses are not flipped.
However, these trends are not reproduced by the other methods (B - G). This suggests that these correlations are also related to the specific algorithm used by Method A to calculate the best-fit deformation gradient tensor, and not only the difference in uncertainty between PC_1 and PC_2.

[1] ε_{13} shear strains very near (approx. < 100 nm from) the edges of SiGe stripes are non-zero due to shear lag relaxations between the SiGe epitaxial thin film and the underlying Si substrate. These strains have been neglected in this study, which used average strains from the interiors of the stripes.

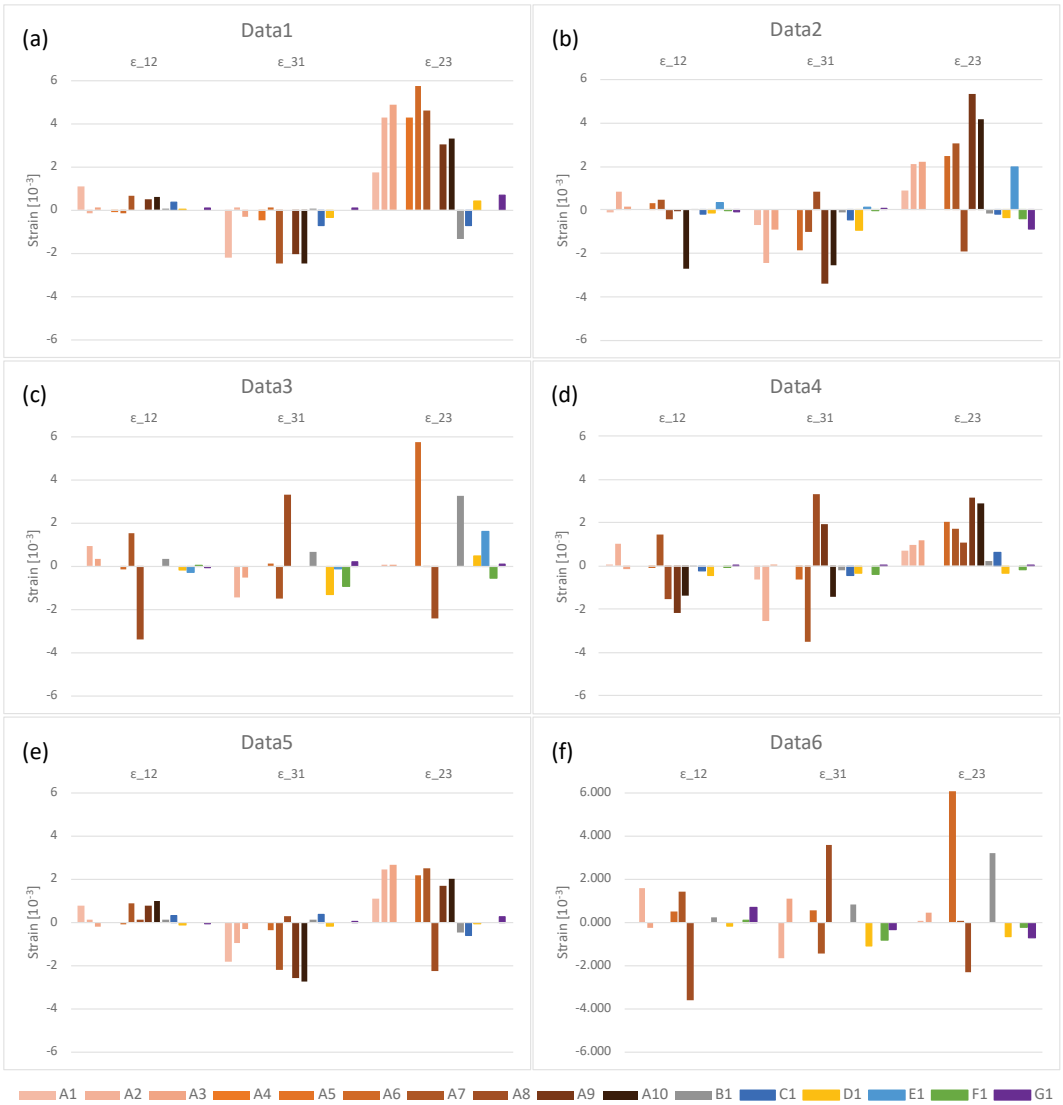

Figure 8: HR-EBSD shear strain components, for all six line scans, plotted on a linear scale.

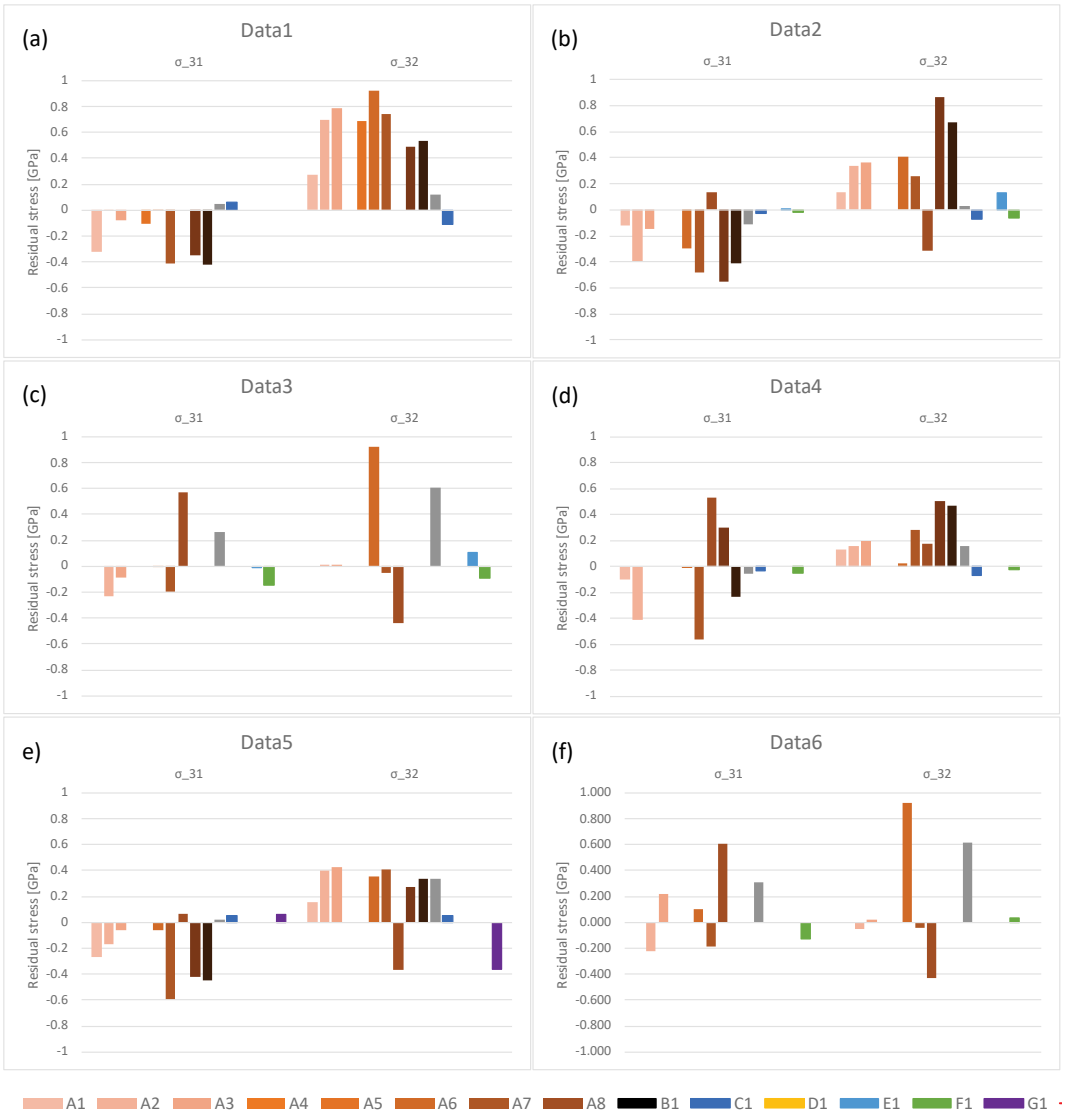

Figure 9: HR-EBSD out-of-plane shear stress components, for all six line scans, plotted on a linear scale.

5 SUMMARY AND RECOMMENDATIONS

5.1 MEASURING AND REPORTING UNCERTAINTY IN HR-EBSD

HR-EBSD elastic strain measurement uncertainty was determined to be on the order of $\pm 10^{-3}$ in this interlaboratory comparison. An uncertainty of $\pm 10^{-3}$ is too close to the elastic limit to resolve the residual stress state of most crystals.
Measurement bias from systematic uncertainties in PC location appears to dominate the HR-EBSD elastic strain uncertainty.

1. A reference material with a strain state of zero (e.g. blank Si wafer) will underestimate strain uncertainty.

2. The out-of-plane shear stress values may be a good estimate of the HR-EBSD stress uncertainty of a given dataset, though this would need an additional step to convert into units of elastic strain, and should be reported alongside HR-EBSD measurements.

5.2 DESIGN OF FUTURE ILC STUDIES

Most participants were not able to return results for all datasets due to difficulties in reading or processing the data in the analysis software. Therefore,

3. HR-EBSD data should be acquired and supplied as an EBSD map (line-scan data as a two- or three-line map), since most analysis programs are primarily designed to handle EBSD maps, and therefore some of software packages did not support handling of line scan data.

4. EBSD data, wherever possible, should be made available in an openly readable format (such as HDF5 binary format, a folder of TIFF images, and/or text files).[12] The EBSD data that were supplied as files in a proprietary binary format could not be read by some participants, in particular those who were developing and maintaining non-commercial software primarily for in-house use. The EBSD community should collectively choose a file format, which could be a specific HDF5 file structure, and encourage hardware and software vendors to use this unified format to enable users to streamline both routine and novel analyses.

Some participants reported results in different units to those specified in the reporting template. These errors are obvious for factors of 10^{-3} in the case of strain vs millistrain, but less obvious for rotations, which can be described in degrees, radians or as direction cosines. The rotation components were not used in the final comparison of results in the current study because of the ambiguity in units. Therefore,

5. The reporting template should allow participants to select their own units and include a blank field for each participant to report the units they used. This would avoid minor errors in the submitted report.

The reporting template contained many fields and was time-consuming for participants to fill in. It was easy for participants to enter a value into the wrong row, and this may not be immediately obvious without detailed inspection of the individual data, particularly for cases where the reference values are identical (e.g. zero). In contrast, the analysed line-scan data returned by each participant were in a variety of different formats, which was time-consuming to load and inspect individually. Therefore,

6. Only one or two simple values per physical parameter (e.g. average and possibly standard deviation) should be requested in the summary report.

7. A spreadsheet template for entering values for individual line scan data should be supplied for returning processed HR-EBSD data.

6 OUTLOOK

Preliminary results were presented to the 2024 ISO TC202 Plenary meeting held in Tokyo. Potential follow-on work based on the results in this report will be discussed at the upcoming 2025 ISO TC202 Plenary meeting. This could include: parametric studies to optimise and guide good practice for the operator-tunable parameters available within ‘Method A’; exploratory studies on the viability of single-material RMs, such as a strained MEMS strain gauge (such as with this example dataset [11]); or a ‘round-robin’ format interlaboratory comparison study to determine reproducibility of HR-EBSD experiments on the same material.

7 ACKNOWLEDGEMENTS

Thanks to all study participants for their time spent on this project, who are listed as authors in alphabetical order. Will Osborn and Mark McLean from NIST provided samples, HR-EBSD data and XRD data, and helpful discussions. The interlaboratory comparison was organised as Project 5 of VAMAS TWA37, led by Dan Hodoroaba. Research was performed in part at the NIST Center for Nanoscale Science and Technology.

8 REFERENCES

[1] A. J. Wilkinson, G. Meaden, and D. J. Dingley, 'High-resolution elastic strain measurement from electron backscatter diffraction patterns: New levels of sensitivity', *Ultramicroscopy*, vol. 106, no. 4–5, pp. 307–313, Mar. 2006, doi: 10.1016/j.ultramic.2005.10.001.

[2] H. Abdolvand and A. J. Wilkinson, 'Assessment of residual stress fields at deformation twin tips and the surrounding environments', *Acta Mater.*, vol. 105, pp. 219–231, Feb. 2016, doi: 10.1016/j.actamat.2015.11.036.

[3] A. Koko, T. H. Becker, E. Elmukashfi, N. M. Pugno, A. J. Wilkinson, and T. J. Marrow, 'HR-EBSD analysis of in situ stable crack growth at the micron scale', *J. Mech. Phys. Solids*, vol. 172, p. 105173, Mar. 2023, doi: 10.1016/j.jmps.2022.105173.

[4] T. B. Britton and A. J. Wilkinson, 'Measurement of residual elastic strain and lattice rotations with high resolution electron backscatter diffraction', *Ultramicroscopy*, vol. 111, no. 8, pp. 1395–1404, 2011, doi: 10.1016/j.ultramic.2011.05.007.

[5] A. Koko, V. Tong, A. J. Wilkinson, and T. J. Marrow, 'An iterative method for reference pattern selection in high-resolution electron backscatter diffraction (HR-EBSD)', *Ultramicroscopy*, vol. 248, p. 113705, Jun. 2023, doi: 10.1016/j.ultramic.2023.113705.

[6] M. D. Vaudin, W. A. Osborn, L. H. Friedman, J. M. Gorham, V. Vartanian, and R. F. Cook, 'Designing a standard for strain mapping: HR-EBSD analysis of SiGe thin film structures on Si', *Ultramicroscopy*, vol. 148, pp. 94–104, Jan. 2015, doi: 10.1016/j.ultramic.2014.09.007.

[7] J. P. Dismukes, L. Ekstrom, and R. J. Paff, 'Lattice Parameter and Density in Germanium-Silicon Alloys[1]', *J. Phys. Chem.*, vol. 68, no. 10, pp. 3021–3027, Oct. 1964, doi: 10.1021/j100792a049.

[8] K. Mingard, A. Day, C. Maurice, and P. Quested, 'Towards high accuracy calibration of electron backscatter diffraction systems', *Ultramicroscopy*, vol. 111, no. 5, pp. 320–329, 2011, doi: 10.1016/j.ultramic.2011.01.012.

[9] J. Alkorta, 'Limits of simulation based high resolution EBSD', *Ultramicroscopy*, vol. 131, pp. 33–38, 2013, doi: 10.1016/j.ultramic.2013.03.020.

[10] T. J. Hardin, T. J. Ruggles, D. P. Koch, S. R. Niezgoda, D. T. Fullwood, and E. R. Homer, 'Analysis of traction-free assumption in high-resolution EBSD measurements', *J. Microsc.*, vol. 260, no. 1, pp. 73–85, Oct. 2015, doi: 10.1111/jmi.12268.

[11] Cios, Grzegorz and Kawałko, Jakub, 'EBSD dataset with patterns (also unprocessed) of strained MEMS device'. doi: 10.5281/zenodo.15633000.

[12] These opinions, recommendations, findings, and conclusions do not necessarily reflect the views or policies of NIST or the United States Government.

9 APPENDIX 1 - HR-EBSD STRAIN MEASUREMENT REPORTING TEMPLATE

HR-EBSD strain measurement comparison

1 INSTRUCTIONS AND INFORMATION

1.1 PARTICIPANT INFORMATION

Name: [Vivian Tong]
Organisation: [NPL]
Date: [2024-07-30]

1.2 EXPERIMENTAL METHOD

Each EBSD dataset is a horizontal line scan across across a set of vertical Si / SiGe stripes on a patterned SiGe on Si chip. The SiGe is strained relative to Si.
For 2-row EBSD maps, please ignore the second row and treat the first row as a line scan.

	Parameter	Value	Notes
1	Dataset name	Data0	
2	Pre-tilt Holder Angle		
3	Stage Tilt Angle		
4	Stage Tilt Axis		
5	Dynamic Focus		
6	Tilt Correction		
7	Camera Insertion Angle		

1.3 DATA FILTERING

Please filter your data into Si and SiGe regions before reporting the strain, and describe your method and/or numbering convention in Table 2.
The first EBSD pattern in the line scan is always Si.
TEMPLATE_hrebsdComparison….docx contains an example of how to fill in Table 2.

Table 2

	Ranges	Notes
Si	[1:19; 37; 39:54; 73:89; 107:125; 142:158; 177:188;]	[Numbers reported as (0_n.tiff) where n=0:189.] [Classified by inspecting and thresholding σ_11: >= -0.5 GPa → Si; <= -0.5 GPa = SiGe.]
SiGe	[20:36; 55:72; 90:106; 125:141; 159:176;]	
Missing data	[37; 189;]	[Experiment file saving error]

2 REPORT

2.1 ANALYSIS METHOD

Please leave irrelevant rows blank and add rows to report any relevant parameters that are not currently included. The parameters below are an example relevant for HR-EBSD analysis in CrossCourt 4.

		Details	Notes / References
1	**Analysis software**	[include version details e.g. CrossCourt version #.#.#.#]	If using in-house written software, please provide a short description of the method and a version identifier, such as a date or Git hash
2	**File format**	[e.g. tif + ctf / h5oina / bcf]	
3	**Stiffness of Si**	[e.g. stiffness matrix constants C11, C12, C44, (used for SiGe too)]	
4	**ROI Size**	[e.g. 20]	
5	**ROI Locations**	[e.g. 1 in centre, 19 in ring around edge]	
6	**Reference Pattern**	[e.g. pattern number and phase]	
7	**Image pre-processing**	[e.g. FFT filter thresholds and cutoff widths, background correction method]	
8	**Data filtering**	[e.g. any excluded data, method to separate SiGe from Si data]	
9	**EBSD Pattern Effective Pixel Size**	[e.g. # µm]	Please calculate this from the Si patterns in this dataset, and use it for beam shift compensation.
10	**Pattern center**	[e.g. [x*, y*, z*] at centre of line scan, as fraction of pattern width, where [0,0,0] = bottom left corner of EBSD pattern]	Please read this value from the EBSD data file and describe how to interpret it.
11	**Line scan step size**	[e.g. # µm]	Please read this value from the EBSD data file.

2.2 RESULTS

Si summary statistics

You should insert your own assumptions about the theoretical values specific to your strain measurement method. Assumptions relevant for the ROI cross-correlation-based HR-EBSD method are provided as an example.
Feel free to add or omit rows and columns if different metrics or summary statistics are relevant for your method.

Table 3

	Metric	Mean	Std Dev	Median	Maximum	Minimum	Gradient / μm^{-1}	Theoretical value
$\times 10^{-3}$	**ε_11**							[= 0 because Si is used as reference pattern]
	ε_22							
	ε_33							
	ε_12							
	ε_31							
	ε_23							
°	**ω_12**							
	ω_23							
	ω_31							
GPa	**σ_11**							
	σ_22							
	σ_12							
	σ_31							[= 0 for a free surface]
	σ_23							[= 0 for a free surface]
	σ_33							[0 - numerically constrained]

SiGe summary statistics

Table 4

	Metric	Mean	Std Dev	Median	Maximum	Minimum	Gradient / μm^{-1}	Theoretical value
$\times 10^{-3}$	**ε_11**							[< 0]
	ε_22							
	ε_33							
	ε_12							
	ε_31							
	ε_23							
°	**ω_12**							
	ω_23							
	ω_31							
GPa	**σ_11**							
	σ_22							
	σ_12							
	σ_31							
	σ_23							
	σ_33							

2.3 REFERENCES

This paper describes the reference material:

[1] Vaudin, M. D., Osborn, W. A., Friedman, L. H., Gorham, J. M., Vartanian, V., & Cook, R. F. (2015). Designing a standard for strain mapping: HR-EBSD analysis of SiGe thin film structures on Si. Ultramicroscopy, 148, 94–104. https://doi.org/10.1016/j.ultramic.2014.09.007

[Add any more if required / used in the previous sections]